Molecular Weight Distribution of a Branched Epoxy Polymer: 1,4-Butanediol Diglycidyl Ether with *cis*-1,2-Cyclohexanedicarboxylic Anhydride

Chi Wu,† Ju Zuo,† and Benjamin Chu*,†,‡

Chemistry Department, State University of New York at Stony Brook, Long Island, New York 11794-3400, and Department of Materials Science and Engineering, State University of New York at Stony Brook, Long Island, New York 11794-3400.
Received December 14, 1987; Revised Manuscript Received June 14, 1988

ABSTRACT: Laser light scattering (LLS) and size exclusion chromatography (SEC) have been used to study the curing of an epoxy resin, 1,4-butanediol diglycidyl ether, with *cis*-1,2-cyclohexanedicarboxylic anhydride. During the curing process, the branched epoxy polymer product formed before its gelation threshold is soluble in either methyl ethyl ketone (MEK) or tetrahydrofuran (THF). LLS could be used successfully to determine the weight-average molecular weight (M_w) and to estimate the molecular weight distribution (MWD) of the branched epoxy polymer at each stage of the polymerization reaction before the gelation threshold. The MWDs obtained from LLS were compared with those determined by conventional SEC. From the comparison, we were able to develop a new absolute calibration procedure for SEC of specific branched polymers. For branched epoxy polymers before its gelation threshold, we were able to confirm the scaling behavior of the size distribution with a critical exponent τ value of 2.1 ± 0.1.

I. Introduction

In recent years, a number of partially conflicting reaction mechanisms have been proposed for the curing process of epoxy resins and anhydrides, with or without triamine as a catalyst.[1] As our knowledge on the molecular structural changes of the polymerization reaction during the curing process is limited, we have focused our attention to study the structure and dynamics of branched epoxy polymer products at different copolymerization stages. Earlier publications[2,3] have detailed the use of fractal geometry to define the random structure formed by the branched epoxy polymer. In this paper, our main objective is to determine the molecular weight distribution (MWD) of the branched epoxy polymer formed during each reaction stage. The procedure is as follows. We first obtained estimates of the normalized characteristic line-width (Γ) distribution function, $G(\Gamma)$, from the measured intensity–intensity time correlation function, $G^{(2)}(\tau)$, by using the Laplace inversion. We then transformed $G(\Gamma)$ to the molecular weight distribution by incorporating information on the static and dynamic properties (i.e. the weight-average molecular weight (M_w), the second virial coefficient (A_2), the diffusion second virial coefficient (k_d), the z-average translational diffusion coefficient at infinite dilute (D_0^0), and the scaling relation $D_0^0 = k_D M^{-\alpha_D}$) of the branched epoxy polymer solution. Knowledge gained from laser light scattering (LLS) of our broad MWD epoxy polymers is sufficient to calibrate the size exclusion chromatographic (SEC) column for branched epoxy polymer studies.

II. Experimental Methods

1. Materials. 1,4-Butanediol diglycidyl ether (DGEB, M_w = 202.3 g/mol) and *cis*-1,2-cyclohexanedicarboxylic anhydride (CH, M_w = 154.2 g/mol) were purchased from Aldrich Chemical Co. and used without further purification since we were able to obtain the same experimental results after both components were purified by vacuum (~0.01 mmHg) distillation. The catalyst (CA), benzyldimethylamine (M_w = 135.2 g/mol), courtesy of Gary L. Hagnauer, Polymer Research Division, Army Materials Technology Laboratory, Watertown, MA) was vacuum distilled before use.

2. Preparation of Solutions. The method of preparation of the reaction mixture has been described in detail elsewhere.[3] The well-mixed reaction mixture containing a molar ratio of epoxy (DGEB):curing agent (CH):catalyst (CA) = 1:2:0.001 was reacted at 80 ± 0.5 °C in an oil bath. Samples containing the epoxy polymer and unreacted monomers (DGEB and CH) were withdrawn from the reaction mixture during the course of the copolymerization process until the gel point was reached. Compositions of the reaction mixture could be analyzed chemically.[4] Portions of withdrawn samples were further dissolved in MEK for LLS measurements and in THF for SEC measurements. Concentrations of the epoxy polymer ranged around 1×10^{-3} g/mL for LLS experiments and 1×10^{-2} g/mL for SEC experiments. Samples for LLS measurements were centrifuged at 7000 gravity and room temperatures for 4 h. A middle portion of the centrifuged solution was then transferred to dust-free cylindrical light scattering cells of 17-mm o.d. by using a dust-free pipet.

3. Methods of Measurement. The light-scattering spectrometer has been described in detail in previous papers.[3,5] It was used for measurements of the angular distribution of absolute scattered intensity as well as its spectral distribution.[5]

For our SEC experiments, we used three ultrastyragel columns designated as 10^2, 10^3, and 10^4 Å (Waters Associates) connected in series, a pump (Waters Model 590) operating at a flow rate of 1.0 mL/min, and a differential refractometer (Waters Model R401) as the detector. The chromatogram was simultaneously recorded on a strip chart recorder and a microcomputer. The sample injection volume was 50 μL with a concentration of ≈1 $\times 10^{-2}$ g/mL, which is below the overloading condition. All SEC experiments were performed at 45 °C in order to increase the efficiency of the columns.

III. Laplace Transform

The MSVD technique[6-8] has been described in detail elsewhere. We outline only the essential steps which are necessary in describing our data fitting results. In the MSVD technique, we do Laplace inversion of the electric field time correlation function

$$g^{(1)}(K,\tau) = \int_0^\infty G(K,\Gamma)e^{-\Gamma(K)\tau}\,d\Gamma \qquad (1)$$

by approximating $G(\Gamma)$ with a set of linearly or logarithmically spaced single exponentials

$$G(\Gamma) = \sum_j P_j \delta(\Gamma - \Gamma_j) \qquad (2)$$

where $g^{(1)}(\tau_i) = b_i = \sum_j P_j \exp(-\Gamma_j \tau_i)$ with P_j being the weighting factors of the δ function measured at scattering vector K. The linear least-squares minimization problem

* To whom all correspondence should be addressed.
† Chemistry Department.
‡ Department of Materials Science and Engineering.

0024-9297/89/2222-0633$01.50/0

has the form $\mathbf{CP} \approx \mathbf{b}$ with the symbol $\approx$ intended to imply solution of the overdetermined set of equations subject to minimization of the Euclidean norm of the residual vector $\|\mathbf{b} - \mathbf{CP}\|$ and the elements of C being $C_{ij} = \exp(\Gamma_j \tau_i)$. The MSVD technique yields a discrete line-width distribution P_js, which can be converted to a continuous line-width distribution. The validity of the MSVD method has been tested previously.[7-10] It should be noted that the procedure we have developed is independent of the method of Laplace inversion. We only used the MSVD technique to demonstrate our approach. Better Laplace inversion techniques should be used when they become available.

IV. Conversion from $G(\Gamma)$ to $F_w(M)$

In previous publications,[8-10] we converted the line-width distribution $G(\Gamma)$ to the weight-average molecular weight distribution $F_w(M)$ by using an experimentally determined scaling relation $\bar{D}_0^0 = k_D M_w^{-\alpha_D}$ where $\bar{D}_0^0$ and M_w are the z-average translational diffusion coefficient extrapolated to infinite dilution and the weight-average molecular weight, respectively. In fact, the Γ to M conversion should use the scaling relation $D_0^0 = k_D M^{-\alpha_D}$ and the condition $\Gamma = DK^2$ based on monodisperse fractions. The k_D and α_D obtained from $\bar{D}_0^0$ and M_w are approximations to the true values since we usually do not have monodisperse polymer samples to establish the scaling relation. In other words, the narrower the molecular weight distributions of calibration samples over the same molecular weight range, the better the approximation becomes. So, the standard calibration method requires a set of narrow molecular weight distribution polymers of different molecular weights. It is very difficult to apply this calibration procedure to study the branched epoxy polymers because all epoxy polymers are very polydisperse and could have different degrees of branching. Thus, we need to examine the calibration problem from a slightly different viewpoint in order to achieve the conversion as precisely as possible. We applied the following procedure for a more precise determination of k_D and α_D.

In the limits $\theta \to 0$ and $C \to 0$, we have $D_0^0 = \Gamma/K^2$, then

$$\int_0^\infty G(D_0^0)\, dD_0^0 \propto \int_0^\infty F_z(M)\, dM \tag{3}$$

where $F_z(M)$ is the z-weighted molecular weight distribution function. By accepting the scaling relation $D_0^0 = k_D M^{-\alpha_D}$, we can rewrite eq 3 to yield

$$\int_0^\infty G(D_0^0)\alpha_D D_0^0\, d[\ln (M)] \propto \int_0^\infty F_z(M) M\, d[\ln (M)] \tag{4}$$

It can be seen from eq 4 that, with the polymer polydispersity being invariant,

$$F_z(M) \propto [G(D_0^0)\alpha_D D_0^0]/M \tag{5}$$

is an acceptable solution. From the definition of M_w, we have

$$M_w = \frac{\int F_w(M) M\, dM}{\int F_w(M)\, dM} \tag{6}$$

where $F_w(M)$ is the mass-weighted molecular weight distribution function and $F_w(M)M = F_z(M)$. In terms of F_z we have

$$M_w = \frac{\int F_z(M)\, dM}{\int [F_z(M)/M]\, dM} \tag{7}$$

By combining eq 5 and 7 with $D_0^0 = k_D M^{-\alpha_D}$, we finally obtain

$$M_w = \frac{k_D^{1/\alpha_D} \int G(D_0^0)\, dD_0^0}{\int G(D_0^0) D_0^{01/\alpha_D}\, dD_0^0} \tag{8}$$

With two polymer samples of different molecular weight and distribution but obeying the same k_D and α_D, we have two $G(D_0^0)$, denoted by $G_1(D_0^0)$ and $G_2(D_0^0)$. From them, we could calculate two $(M_w)_{calcd}$, denoted by $(M_{w,1})_{calcd}$ and $(M_{w,2})_{calcd}$. The ratio of $(M_{w,1})_{calcd}$ and $(M_{w,2})_{calcd}$ is

$$\frac{(M_{w,1})_{calcd}}{(M_{w,2})_{calcd}} = \frac{\left[\int G_1(D_0^0)\, dD_0^0\right]\left[\int G_2(D_0^0) D_0^{01/\alpha_D}\, dD_0^0\right]}{\left[\int G_2(D_0^0)\, dD_0^0\right]\left[\int G_1(D_0^0) D_0^{01/\alpha_D}\, dD_0^0\right]} \tag{9}$$

where k_D has been cancelled out. The two calculated $(M_w)_{calcd}$ values have to equal the two measured M_w values. It means that we already know the value of left side of eq 9 experimentally. Now, we vary the value of α_D and calculate the right side of eq 9 until the left side equals to the right side. In this way, we are able to find the correct α_D value from two polymer samples with different and broad MWD. After we have determined α_D, we can determine the k_D value by using eq 8. The above procedure can be expanded easily to N samples of different molecular weight and distribution. After having determined the correct values of k_D and α_D, we can use eq 5 and the scaling relation $D_0^0 = k_D M^{-\alpha_D}$ (not $\bar{D}_0^0 = k_D M_w^{-\alpha_D}$) to convert $G(D_0^0)$ versus D_0^0 to $F_w(M)$ versus M.

V. SEC Calibration

There are many calibration methods for the SEC column.[11-21] However, for branched polymers and rodlike polymers, conventional calibration methods do not apply. All reported calibration methods require at least two polymers with different molecular weights, or one sample with either two different molecular weight averages or one molecular weight plus intrinsic viscosity data, implying the use of one more instrument, such as an osmometer or a viscometer. In laser light scattering, we need only one broad MWD polymer sample and one instrument (i.e. LLS) to calibrate the SEC column.

We outline our conversion method for getting the molecular weight distribution of epoxy polymers from SEC as follows. For SEC experiments, the elution volume V and the polymer molecular weight has the relation

$$V = A + B \log (M) \tag{10}$$

By taking the logarithm of both sides of the scaling relation $D_0^0 = k_D M^{-\alpha_D}$ and substituting D for M in eq 10, we obtain

$$V = \mathbf{A} + \mathbf{B} \log (D_0^0) \tag{11}$$

where $\mathbf{A} = A + [B \log (k_D)]/\alpha_D$ and $\mathbf{B} = -B/\alpha_D$. By squaring both sides of eq 11, we have

$$V^2 = \mathbf{A}^2 + 2\mathbf{AB} \log (D_0^0) + \mathbf{B}^2 \log^2 (D_0^0) \tag{12}$$

Further, we average both sides of eq 11 and 12 to obtain

$$\langle V \rangle = \mathbf{A} + \mathbf{B} \langle \log (D_0^0) \rangle \tag{13}$$

and

$$\langle V^2 \rangle = \mathbf{A}^2 + 2\mathbf{AB} \langle \log (D_0^0) \rangle + \mathbf{B}^2 \langle \log^2 (D_0^0) \rangle \tag{14}$$

where $\langle\ \rangle$ is the symbol denoting an average. From SEC measurements, we can obtain the elution curve $C(V)$ versus

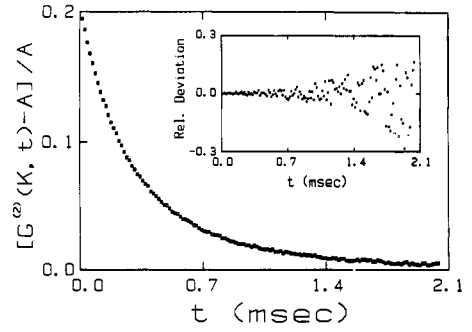

Figure 1. A typical unnormalized intensity–intensity photoelectron count autocorrelation function. Epoxy polymer sample 13 (1.11×10^{-4} g/mL; $M_w = 4.97 \times 10^5$) in MEK measured at $\theta = 30°$ and 25 °C using a delay time increment $\Delta\tau = 15$ μs. The insert is relative deviation of the measured and the computed time correlation function using the MSVD method. Relative deviation is defined as $1 - [b|g^{(1)}(t)|^2]_{calcd}/[b|g^{(1)}(t)|^2]_{measd}$.

V, which can be used to calculate $\langle V \rangle$ and $\langle V^2 \rangle$ by using $\langle V \rangle = \int_0^\infty VC(V)\,dV$ and $\langle V^2 \rangle = \int_0^\infty V^2C(V)\,dV$. From laser light scattering, we can obtain the line-width distribution $G(\Gamma)$ versus Γ, which can be converted to $G(D_0^0)$ versus D_0^0 and used to calculate $\langle \log (D_0^0) \rangle$ and $\langle \log^2 (D_0^0) \rangle$ by using $\langle \log (D_0^0) \rangle = \int_0^\infty \log (D_0^0) G(D_0^0)\,dD_0^0$ and $\langle \log^2 (D_0^0) \rangle = \int_0^\infty \log^2 (D_0^0) G(D_0^0)\,dD_0^0$. After obtaining $\langle V \rangle$, $\langle V^2 \rangle$, $\langle \log (D_0^0) \rangle$, and $\langle \log^2 (D_0^0) \rangle$, we can combine them with eq 13 and 14 to solve for **A** and **B**. We also know that M_w can be calculated from SEC data by using

$$M_w = \frac{\int_0^\infty MC(V)\,dV}{\int_0^\infty C(V)\,dV} \tag{15}$$

if we know A and B in eq 10. By using $D_0^0 = k_D M^{-\alpha_D}$, **A**, and **B**, we can change eq 15 to

$$M_w = \frac{k_D^{1/\alpha_D} \int_0^\infty 10^{(A-V)/(\alpha_D B)} C(V)\,dV}{\int_0^\infty C(V)\,dV} \tag{16}$$

The molecular weights calculated from eq 8 and eq 16 have to equal; i.e., we have

$$1 = \frac{\left[\int_0^\infty 10^{(A-V)/(\alpha_D B)} C(V)\,dV\right]\left[\int_0^\infty G(D_0^0) {D_0^0}^{1/\alpha_D}\,dD_0^0\right]}{\left[\int_0^\infty C(V)\,dV\right]\left[\int_0^\infty G(D_0^0)\,dD_0^0\right]} \tag{17}$$

There is only one unknown value for α_D in eq 17. We can vary the value of α_D and calculate the value of the right side of eq 17 until it equals to 1. In this way, we will be able to find the correct value of α_D. After having determined α_D, we can easily calculate k_D from eq 16 or eq 8 by using the M_w obtained from the same laser light scattering instrument. Then, we can find A and B in eq 10 by using **A**, **B**, k_D, and α_D.

VI. Results and Discussion

By following the experimental procedures for self-beating and base-line considerations, we could obtain precise measurements of the intensity–intensity time correlation function $G^{(2)}(K,\tau)$

$$G^{(2)}(K,\tau) = A(1 + b|g^{(1)}(K,\tau)|^2) \tag{18}$$

where the base-line A agreed with the measured base-line $\lim_{\tau\to\infty} G^{(2)}(K,\tau)$ to within about 0.1%. Figure 1 shows a typical experimental intensity–intensity photoelectron count autocorrelation function for the epoxy polymer in MEK measured at $\theta = 30°$ and 25 °C using a delay time increment $\Delta\tau$ of 15 μs and relative deviation of the measured and the computed time correlation function by using the MSVD method of Laplace inversion. We have to stress here that, in an ill-posed problem, goodness of fitting does not guarantee a correct solution to the inversion. However, the validity of the MSVD method for a unimodal characteristic line-width distribution has been tested thoroughly by using simulated data and known polymer systems under comparable experimental conditions, counting rates, and statistics. Figure 2 shows typical line-width distributions obtained by the MSVD method. In Figure 2, we clearly see that the characteristic line-width shifts to lower frequencies and the distributions become narrower with increasing percent of conversion. Numerical results of the transform by the MSVD method for a set of epoxy polymers at different percent conversions are listed in Table I. It should be noted that discrete (P_js) and continuous ($G(\Gamma)$) normalized characteristic line-width distributions are not the same. In a discrete distribution in terms of P_js, we have eq 2. If Γ_j does not have equal spacing, which is indeed the case for our MSVD method, P_j has to be rescaled in order to convert it to a continuous distribution $G(\Gamma)$; i.e., $G(\Gamma) \neq G(\ln \Gamma)$. The rescaling is approximately done by using $G(\Gamma_j) = P_j/\Gamma_j$.

In order to transform the measured characteristic line-width distribution at finite angle and finite concentration to a molecular weight distribution, we have to know how the characteristic line-width Γ depends on the scattering

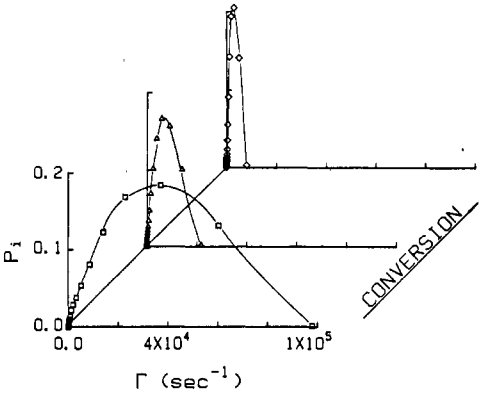

Figure 2. Plots of P_j versus Γ for epoxy polymer sample 1, sample 9, and sample 13 in MEK at $\theta = 30°$ and 25 °C based on the MSVD method (sample, notation, M_w (g/mol), $\bar{\Gamma}$ (s^{-1}), $\mu_2/\bar{\Gamma}^2$): 1, hollow squares, 4.32×10^3, 2.29×10^4, 0.63; 9, hollow triangles, 1.03×10^5, 3.98×10^3, 0.45; 13, hollow diamonds, 4.97×10^5, 1.79 $\times 10^3$, 0.40.

Table I
Experimental Results Based on the MSVD Method for the Epoxy Polymer Samples in MEK at 25 °C and $\lambda_0 = 488$ nm

sample	conversn (CH %)	M_w (g/mol)	$\bar{D}_0^0$ (cm^2/s)	$\mu_2/\bar{\Gamma}^2$	f	k_d (mL/g)
1	6.5	4.32×10^3	2.71×10^{-6}	0.63		0
2	13.3	6.14×10^3	2.27×10^{-6}	0.61		11
3	20.0	8.23×10^3	1.77×10^{-6}	0.56		16
4	26.5	1.25×10^4	1.29×10^{-6}	0.53		22
5	33.5	2.11×10^4	1.00×10^{-6}	0.51		29
6	36.0	3.37×10^4	7.98×10^{-7}	0.48		36
7	38.5	5.00×10^4	6.45×10^{-7}	0.47	0.15	48
8	40.0	7.68×10^4	5.26×10^{-7}	0.46	0.17	63
9	41.0	1.03×10^5	4.38×10^{-7}	0.45	0.13	79
10	42.5	1.42×10^5	3.68×10^{-7}	0.43	0.18	89
11	44.0	2.19×10^5	2.97×10^{-7}	0.40	0.21	101
12	45.3	3.01×10^5	2.60×10^{-7}	0.42	0.16	132
13	46.5	4.97×10^5	2.05×10^{-7}	0.40	0.19	141

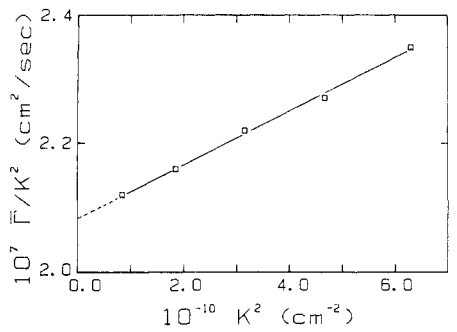

Figure 3. Plots of $\bar{\Gamma}/K^2$ versus K^2 for epoxy polymer 13 (M_w = 4.97 × 10^5 and $\langle R_g^2\rangle_z^{1/2}$ = 31.4 nm) in MEK at 25 °C and λ_0 = 488 nm. The straight line represents $\bar{\Gamma}/K^2 = 2.08 \times 10^{-7}(1 + 0.19\langle R_g^2\rangle_z K^2)$.

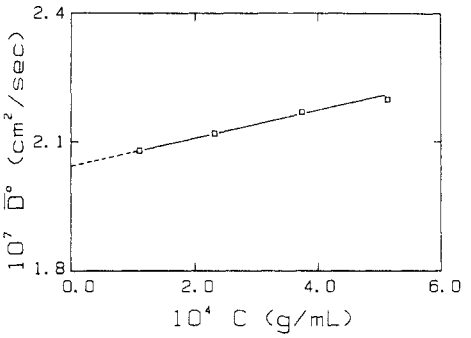

Figure 4. Plots of $\bar{D}^0$ (= $\lim_{K\to 0} \bar{\Gamma}/K^2$) versus concentrations (C) for the same sample in Figure 3. The straight line represents $\bar{D}^0 = 2.05 \times 10^{-7}(1 + 1.41 \times 10^2 C)$.

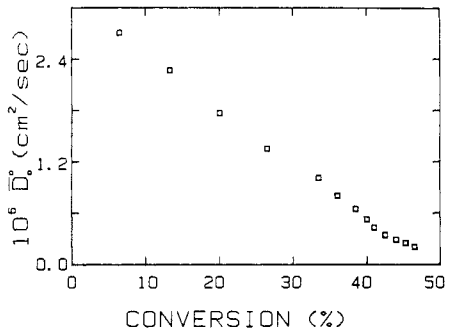

Figure 5. Plot of z-average translational diffusion coefficient at infinite dilution $\bar{D}_0^0$ versus extent of conversion (100$[CH]_t$/$[CH]_0$%) where $[CH]_t$ is the molar concentration of CH at time $t = t$ and $[CH]_0$ is molar concentration of CH at time $t = 0$.

angle (or K) and the polymer concentration. We experimentally determined such a relation by using

$$\bar{\Gamma} = \bar{D}_0^0 K^2(1 + f\langle R_g^2\rangle_z K^2)(1 + k_d C) \qquad (19)$$

where f is a dimensionless number and depends on chain structure, polydispersity and solvent quality, k_d is the second virial coefficient for diffusion, and $\langle R_g^2\rangle_z$ is the z-average mean square radius of gyration. Figure 3 shows a typical K^2 dependence of the z-average characteristic line-width $\bar{\Gamma}$. Figure 4 shows a typical concentration dependence of the translational diffusion coefficient $\bar{D}^0$ (= $\lim_{K\to 0} \bar{\Gamma}/K^2$). The k_d and f values are also listed in Table I. After having obtained k_d and f, we can convert $G(\Gamma)$ versus Γ to $G(D_0^0)$ versus D_0^0. Further, we can calculate the z-average translational diffusion coefficient $\bar{D}_0^0$ at each reaction stage, as shown in Figure 5. By using the $\bar{D}_0^0$ and the Stokes–Einstein relation: $D = k_B T/6\pi\eta R_h$, we can calculate the equivalent hydrodynamic radius R_h.

By measuring the angular dependence of the excess absolute integrated intensity of light scattered by a dilute epoxy polymer solution, we can determine the weight-average molecular weight M_w and the z-average root-mean-square radius of gyration $\langle R_g^2\rangle_z^{1/2}$ at each reaction stage up to the gel point. Figure 6 shows how M_w changes with the extent of the polymerization reaction. A log–log plot of $\bar{D}_0^0$ versus M_w is shown in Figure 7. We find that the data can be represented by a straight line if we disregard the first three data points during the initial stages of the curing process. Why do the first three points behave differently from the rest of data points? During the initial reaction stage, the molecular weights of the epoxy polymer formed are small (below 10^4). Our results also suggest that the initial epoxy polymers are less highly branched. From Figure 7, we calculated $k_D = (1.56 \pm 0.20) \times 10^{-4}$ and $\alpha_D = 0.508 \pm 0.011$ with $\bar{D}_0^0$ and M_w expressed in units of cm^2/s and g/mol, respectively. By using the method presented in section III, we obtained that $k_D = (2.14 \pm 0.32) \times 10^{-4}$ and $\alpha_D = 0.527 \pm 0.013$. The k_D and α_D obtained from average values of M_w and $\bar{D}_0^0$, as shown in Figure 7, are different from the results obtained from M and D_0^0. It is not surprising because our branched epoxy polymers are quite polydisperse.

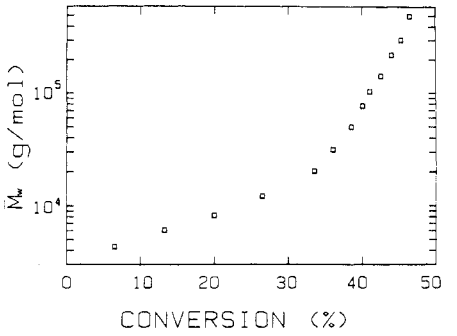

Figure 6. Plots of weight-average molecular weight M_w versus extent of conversion (100$[CH]_t$/$[CH]_0$%).

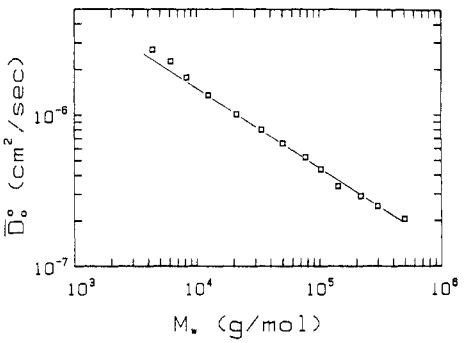

Figure 7. log–log plot of translational diffusion coefficient $\bar{D}_0^0$ versus M_w for the epoxy polymer in MEK at 25 °C and λ_0 = 488 nm. The straight line represents $\bar{D}_0^0 = 1.56 \times 10^{-4} M_w^{-0.508}$ with $\bar{D}_0^0$ and M_w in units of cm^2/s and g/mol, respectively.

Having computed $G(D_0^0)$ versus D_0^0, we now make use of the relation for the translational diffusion coefficient $D_{0,j}^0$ (in cm^2/s) = $2.14 \times 10^{-4} M_j^{-0.527}$ for each fraction of the epoxy polymer having molecular weight M_j (in g/mol). At each scattering angle, the excess Rayleigh ratio has the form

$$R_{vv}(K) \propto \sum_j F_w(M_j) M_j P(M_j,K) \propto \sum_j P_j \qquad (20)$$

where $P(M,K)$ is the particle scattering factor and $F_w(M)$ is the normalized weight distribution for the epoxy polymers. The $\propto$ sign denotes that we are not concerned with the proportionality constant. At small enough scattering angles, $P_j \propto F_w(M_j) M_j P(M_j,K) \approx F_w(M_j) M_j$ as $P(M_j,K) \approx 1$. The first-order term for $P(M_j,K)$ has the form $P(M_j,K) \approx 1 - \langle R_g^2\rangle_{z,M_j} K^2/3$. Thus, we can correct for the interference effect in the molecular weight distribution when-

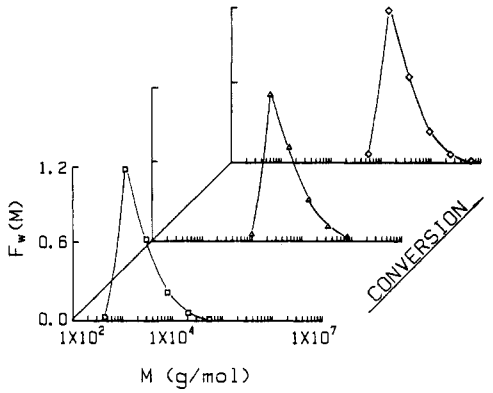

Figure 8. Typical plots of approximate weight distributions for the same samples in Figure 2 (sample, notation, M_w (g/mol), M_n (g/mol), M_w:M_n): 1, hollow squares, 4.32×10^3, 1.30×10^3, 3.32; 9, hollow triangles, 1.03×10^5, 3.99×10^4, 2.58; 13, hollow diamonds, 4.97×10^5, 2.00×10^5, 2.49.

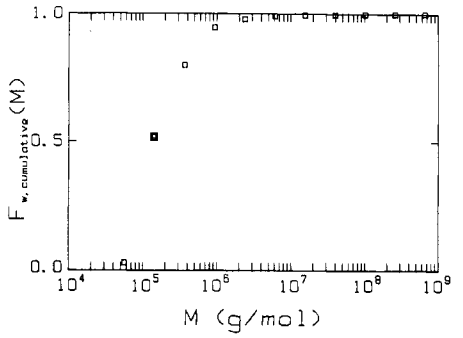

Figure 9. Cumulative molecular weight distribution for the epoxy polymer sample 13 ($M_w = 4.97 \times 10^5$) measured in MEK at 25 °C and $\lambda_0 = 488$ nm, which is defined as $F_{w,cumulative} = \int_0^M F_w(M)\, dM$.

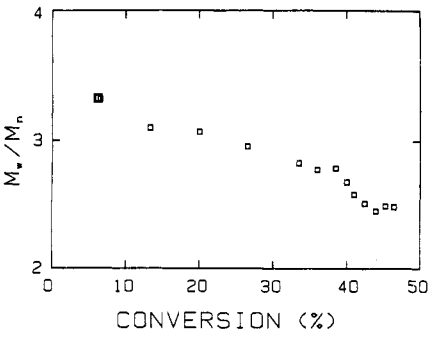

Figure 10. Plot of M_w/M_n versus extent of conversion for 13 epoxy polymers at different reaction stages. M_w/M_n were determined by using the MSVD method.

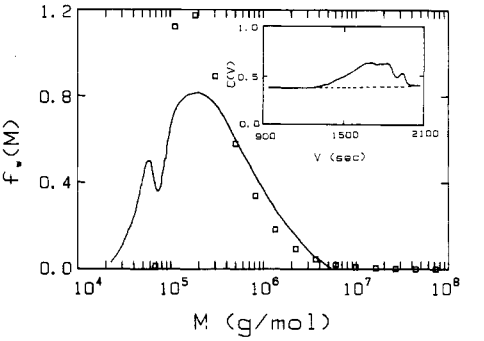

Figure 11. Comparison of the weight distributions $F_w(M)$ obtained for the same epoxy polymer ($M_w = 4.97 \times 10^5$ g/mol) by using the SEC experiment (continuous line) and the LLS experiment (hollow squares). Inset: typical SEC curve of the epoxy polymer ($M_w = 4.97 \times 10^5$ g/mol) measured at a flow rate of 1 mL/min and 45 °C using a Waters R401 differential refractometer as the concentration detector. The output was recorded on a 64K Morrow microcomputer through an IEEE interface and signal averaged.

ever it is necessary since we have the empirical scaling relation between the radius of gyration and the molecular weight.[3]

Figure 8 shows three typical normalized weight distributions of the epoxy polymers at three different percent conversions. In Figure 8, we have ignored the very high molecular weight tails on the distribution curves because of noise and background uncertainties. The contribution of the high molecular weight tail to the cumulative molecular weight distribution is less than 1% of the total weight fraction as shown clearly in Figure 9. From the $F_w(M)$ distributions, we can calculate M_w:M_n, which represents the polydispersity of each epoxy polymer sample. The results of M_w:M_n for 13 samples at different percent conversion are shown in Figure 10. It is noted that the values of M_w:M_n become smaller with increasing reaction time, suggesting that the polydispersity of the branched epoxy polymer product during the initial stages is much higher than that at the later stages near the gelation threshold. We also observed that M_w:M_n approaches a constant value of $\approx$2.5 as the polymerization approaches the gelation threshold.

In order to check our determination of the molecular weight distribution by means of LLS, we used the same samples for SEC experiments. The method to calibrate the SEC column has already been described in section V. In the SEC experiment, the elution volume V and the elution curve $C(V)$ were recorded, respectively, as an elution time (in units of s) and a dc voltage (in units of mV) on a 64K MORROW microcomputer through the IEEE interface. A typical elution curve is shown in the inset of Figure 11. By using the method in section V, we obtained $A = (5.48 \pm 0.55) \times 10^3$ (s) and $B = -(5.83 \pm 0.27) \times 10^2$ in V (s) = $A + B \log (M)$. We also determined $k_D = (1.92 \pm 0.15) \times 10^{-4}$ and $\alpha_D = 0.521 \pm 0.015$ in $D_0^0 = k_D M^{-\alpha_D}$. The k_D and α_D values determined from this procedure were very close to the values obtained by using the method described in section III. It confirmed the validity of k_D and α_D values which we used to convert the line-width distribution to the molecular weight distribution. The influence of experimental error in LLS data on the parameters A and B in eq 10 was tested by arbitrarily varying the M_w and D_0^0. We found that A varied in the same order as M_w while the parameter B varied less. If we take the experimental errors of M_w and D_0^0 to be 5–10% and a few percent, respectively, the final estimated errors from A and B should be $\lesssim$20% and 10%, respectively.

In our analysis, we have also considered the polydisperse nature of the epoxy polymer products. By fractionating four epoxy polymer products from different extent of conversion, we obtained a new set of (four) fractionated epoxy polymers, each having a narrower MWD and a slightly different M_w from the original unfractionated set. The weight-average molecular weight M_w and the polydispersity index M_w/M_n were again determined by using LLS with M_w and M_w/M_n values of 4.92×10^4 and 1.53, 2.34×10^5 and 1.62, 5.93×10^5 and 1.57, 1.79×10^6 and 1.71, respectively. From the fractionated set, we also determined $\bar{D}_0^0 = 1.74 \times 10^{-4} M_w^{-0.514}$ and $\bar{V} = 5.71 \times 10^3 - 6.03 \times 10^2 \log (M_w)$. The results are tabulated in Table II, showing fairly good agreement between the two data sets. After having determined the values of A and B, a plot of the elution curve, $C(V)$ versus V, can easily be transformed to $F_w(M)$ versus M. Figure 11 shows plots of $F_w(M)$ versus M with $F_w(M)$ from SEC denoted by the continuous line

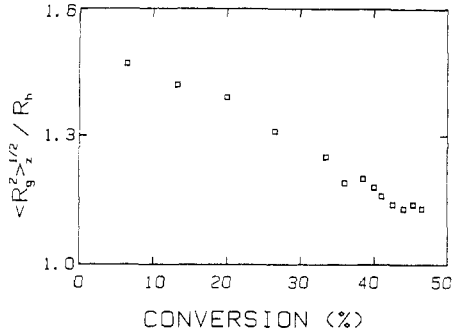

Figure 12. Plot of $\langle R_g^2\rangle_z^{1/2}/R_h$ for 13 epoxy polymer samples at different reaction stages.

Table II
Comparison of Parameters for Polydisperse and Fractionated Epoxy Polymers

	unfractionated ($M_w/M_n \approx 2.5$–3.4) (method in IV)	unfractionated ($M_w/M_n \sim 2.5$–3.4) (log $\bar{D}_0^0$ or $\bar{V}$ versus log M_w)
k_D	$(2.14 \pm 0.32) \times 10^{-4}$	$(1.56 \pm 0.20) \times 10^{-4}$
α_D	0.527 ± 0.013	0.508 ± 0.011
	unfractionated ($M_w/M_n \sim 2.5$–3.4) (method in V)	fractionated ($M_w/M_n \sim 1.5$–1.7) (log $\bar{D}_0^0$ or $\bar{V}$ versus log M_w)
k_D	$(1.92 \pm 0.15) \times 10^{-4}$	$(1.74 \pm 0.19) \times 10^{-4}$
α_D	0.521 ± 0.015	0.514 ± 0.021
A	$(5.48 \pm 0.55) \times 10^3$	$(5.71 \pm 0.42) \times 10^3$
B	$-(5.83 \pm 0.27) \times 10^2$	$-(6.03 \pm 0.34) \times 10^2$

and those from LLS denoted by hollow squares. The agreement is reasonable especially if we take into account of the facts that LLS emphasizes on larger particles and SEC emphasizes on particle weight fractions. $F_w(M)$ from SEC showed a small peak around molecular weight 6×10^3, which was not observed in $F_w(M)$ from LLS. This discrepancy is not surprising because signals from LLS not only emphasized large particles, but our MSVD Laplace inversion technique is designed for unimodal characteristic line-width distribution analysis. We also tried to use the CONTIN algorithm which could resolve the bimodal character if the intensity contributions of both peaks were above the noise. In Figure 11, we noted an estimated intensity ratio of only a few percent for the small to large peak ratio from SEC. With a molecular weight separation of about a factor of 4 for the two peaks, it is reasonable to find that LLS cannot resolve the two peaks. The low molecular weight peaks as revealed by SEC tells us additional kinetics information about the formation of the epoxy polymer network, which will be discussed in a separate paper. By comparing the two MWDs from LLS and SEC, we note that M_w:M_n (≈ 3.0) by SEC is larger than the value (≈ 2.5) obtained from LLS.

Figure 12 shows the ratios of the z-average root-mean-square radius of gyration and the hydrodynamic radius,[22] $\rho = R_g/R_h$, for the 13 epoxy polymer samples which we extracted during different reaction stages. ρ does not depend on the bond length and the degree of copolymerization but is a function of the branching density and polydispersity. For a linear polymer coil, $R_g/R_h \approx 1.504$. For a highly branched polymer with a monodisperse primary coil chain distribution, the value of R_g/R_h decreases to 1.130.[23,24] In Table I of ref 23, the calculated values of ρ changed from 1.5044 to 1.1657 for polymers with the degree of branching changed from 1 (linear polymer) to 100, respectively. The value of R_g/R_h ratio obtained from our experimental results changed from 1.47 to 1.14 as the reaction approaches the gel point. The change in R_g/R_h ratio tells us that the epoxy polymer behaves close to a linear random coil during the initial reaction stages. The degree of branching increases as the polymerization reaction approaches the gel point.

The evolution of the molecular weight distribution function during the gelation transition is related to the spectacular variation of macroscopic properties of a cross-linked polymer system.[25,26] There are only small molecules inside the reaction bath at the initial reaction stage. Near the gelation threshold, a macroscopic cluster as well as precursor units and clusters of all intermediate sizes are formed. Various statistical and kinetic models have been proposed to describe the evolution of the molecule weight distribution for different gelation processes.[25-30] They all show that the molecular weight distribution of large clusters near the gelation threshold can be written in a scaling form[31]

$$N(M,\epsilon) \approx M^{-\tau} f(M/M^*(\epsilon)) \tag{21}$$

where $N(M,\epsilon)$ is the number of clusters with molecular weight M when the relative distance from the gel point is ϵ. $\epsilon = |p - p_c|$, where p is the extent of conversion and p_c is the extent of conversion at the gelation threshold. Equation 21 implies that the number of clusters decreases as a power law of molecular weight with a critical exponent τ. Before the gelation threshold, a typical molecular weight $M^*(\epsilon)$ exists in the molecular weight distribution, which limits the spread of the distribution and which diverges when the gel threshold is approached: $M^* \approx \epsilon^{-1/\sigma}$, where $1/\sigma$ is a constant which is sometimes referred to as the gap exponent. The crossover function $f(x)$ describes the cutoff of the distribution for large molecules greater than M^*. L. Leibler and F. Schosseler experimentally demonstrated[32] a direct quantitative method of measuring the typical molecular weight (M^*) from light-scattering spectra. They showed that the molecular weight M_{max} of molecules in the distribution given the maximum scattered light intensity provides a measure of the cutoff molecular weight and can be identified with the typical molecular weight M^*. They also experimentally showed that if eq 21 holds for the molecular weight distribution of branched polymer molecules, the function

$$G(M/M_{max}) = M_{max}^{\tau-1}\phi(M,t) \approx (M/M_{max})^{1-\tau} f(M/M_{max}) \tag{22}$$

is a universal function of M/M_{max} independent of the advancement of the reaction, t. Equation 22 is valid for the high molecular weight M for which $\phi(M,t)$ is expected to be independent of the initial molecular weight distribution, τ in eq 22 cannot take an arbitrary value since eq 22 implies that the weight-average molecular weight M_w varies like $M_{max}^{3-\tau}$.

From the light scattering theory, we know that the scattered intensity (I) can be written as

$$I = \int_0^\infty I(M)\, dM \propto \int_0^\infty f_n(M) M^2\, dM = \int_0^\infty f_z(M)\, dM \tag{23}$$

where $I(M)$ is the scattered intensity from the fraction of polymer with molecular weight M. Equation 23 tells us that $(I(M))_{max}$ corresponds to $(f_z(M))_{max}$ as shown in Figure 13. Then, the molecular weight M corresponding to $(f_z(M))_{max}$ should be M_{max}. Experimentally, we measured M_w and calculated $f_z(M)$ from the line-width measurements for different reaction stages. We obtained M_{max} from $(f_z(M))_{max}$ in the distribution. A log–log plot of M_{max} versus M_w is shown in Figure 14. The data points except the first three lower molecular weight values are essentially on a straight line, whose slope is 1.1 ± 0.1. From the slope, we

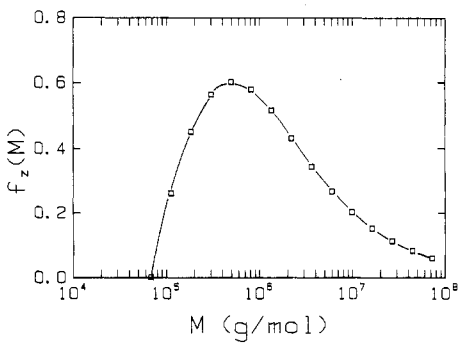

Figure 13. Plot of $f_z(M)$ versus M, based on $F_w(M)$ versus M data from LLS in Figure 12. M_{max} is determined from the location of M at which $(f_z(M))_{max}$ occurs.

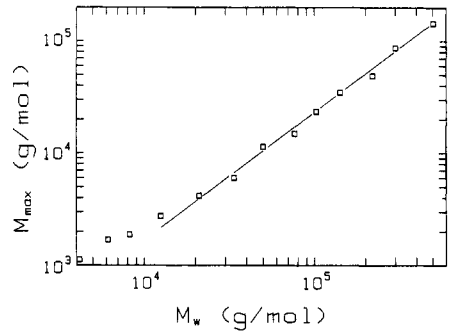

Figure 14. log–log plot of M_{max} versus M_w. Slope = $(3 - \tau)^{-1}$ = 1.1 ± 0.1 and τ = 2.1 ± 0.1.

calculated τ = 2.1 ± 0.1. The result further confirms the existence of a scaling law for the molecular weight distribution function in the sol phase, the main result of all theories concerned with gelation processes. Our value of the scaling constant τ is smaller than the classical mean-field prediction τ = 2.5 but is close to the value of 2.3 in ref 32.

VII. Conclusions

Laser light scattering, including measurements of angular distribution of absolute scattered intensity and of time correlation function together with correlation function profile analysis, has been developed into a powerful analytical tool for branched epoxy polymer characterizations. We have succeeded in determining the molecular weight and its distributions of branched epoxy polymers during its curing process. From the molecular weight distribution at each reaction stage, we have been able to establish a new calibration method to analyze the branched epoxy polymers. By using the LLS approach described in this paper, we can study how temperature, composition, and catalyst effect the epoxy polymerization process and determine the molecular weight distribution at different reaction stages without relying on the more tedious analytical technique of size exclusion chromatography. Experimentally, we have further shown that there exists a scaling relationship for the molecular weight distribution in the sol phase of the cross-linked epoxy–anhydride system. The scaling constant τ (= 2.1 ± 0.1) is very close to our previously determined fractal dimension d_f (= 2.17 ± 0.05).

Acknowledgment. We gratefully acknowledge support of this work by the U.S. Army Research Office (DAAG2985K0067).

Registry No. (DGEB)(CH) (copolymer), 113810-65-4.

References and Notes

(1) See, for example: Antoon, M. K.; Koenig, J. L. *J. Polym. Sci., Polym. Chem. Ed.* **1981**, *19*, 549 and references therein.
(2) Chu, B.; Wu, C.; Wu, D.-Q.; Phillips, J. C. *Macromolecules* **1987**, *20*, 2642.
(3) Chu, B.; Wu, C. *Macromolecules*, in press.
(4) May, C. A.; Tanaka, Y. *Epoxy Resins Chemistry and Technology*; Marcel Dekker: New York, 1973; p 683.
(5) Chu, B.; Wu, C. *Macromolecules* **1987**, *20*, 93.
(6) See: *Proceedings of the 5th International Conference on Photon Correlation Techniques in Field Mechanics*, Springer Series in Optical Sciences; Schulz-DuBois, E. O., Ed.; Springer-Verlag: New York, 1983.
(7) Chu, B.; Ford, J. R.; Dhadwal, H. S. *Methods Enzymol.* **1985**, *117*, 256–297.
(8) Chu, B.; Ying, Q.-C.; Wu, C.; Ford, J. R.; Dhadwal, H. S. *Polymer* **1985**, *26*, 1408.
(9) Wu, C.; Buck, W.; Chu, B. *Macromolecules* **1987**, *20*, 98.
(10) Chu, B.; Wu, C.; Buck, W. *Macromolecules*, in press.
(11) Grubisic, Z.; Rempp, P.; Benoit, H. *J. Polym. Sci., Part B* **1967**, *5*, 753–759.
(12) Moore, J. C.; Hendrickson, J. G. *J. Polym. Sci., Part C* **1965**, *8*, 233–241.
(13) Mori, S. *J. Chromatogr.* **1978**, *157*, 75–84.
(14) Mori, S. *J. Appl. Polym. Sci.* **1974**, *18*, 2391–2397.
(15) Loy, B. R. *J. Polym. Sci., Polym. Chem. Ed.* **1976**, *14*, 23.
(16) Vrijbergen, R. R.; Soeteman, A. A.; Smit, J. A. M. *J. Appl. Polym. Sci.* **1978**, *22*, 1267–1276.
(17) McCrackin, F. L. *J. Appl. Polym. Sci.* **1977**, *21*, 191–198.
(18) Mahabadi, H. K.; O'Driscoll, K. F. *J. Appl. Polym. Sci.* **1977**, *21*, 1283–1287.
(19) Weiss, A. R.; Cohn-Ginsberg, E. *J. Polym. Sci., Part B* **1969**, *7*, 379–381.
(20) Mori, S. *Anal. Chem.* **1981**, *53*, 1813–1818.
(21) Hamielec, A. E.; Omorodion, S. N. E. *ACS Symp. Ser.* **1980**, *No. 138*, 183–196.
(22) Burchard, W.; Schmidt, M.; Stockmayer, W. H. *Macromolecules* **1980**, *13*, 1265.
(23) Kajiwara, K.; Burchard, W. *Polymer* **1981**, *22*, 1621.
(24) Gordon, M. *Proc. R. Soc. London* **1962**, *268*, 240.
(25) Flory, J. *J. Am. Chem. Soc.* **1941**, *63*, 1096, 3083, 3091.
(26) Stockmayer, W. H. *J. Chem. Phys.* **1944**, *12*, 125.
(27) de Gennes, P. G. *Scaling Concepts in Polymer Physics*, Cornell University: Ithaca, NY, 1979.
(28) Stauffer, D.; Coniglio, A.; Adam, M. *Adv. Polym. Sci.* **1982**, *44*, 103.
(29) Ernst, M. H.; Ziff, R. M.; Hendriks, E. M. *J. Colloid Interfacial Sci.* **1984**, *97*, 266.
(30) Herrmann, H.; Landau, D. P.; Stauffer, D. *Phys. Rev. Lett.* **1983**, *49*, 412.
(31) Stauffer, D. *Phys. Rep.* **1979**, *54*, 1.
(32) Leiber, L.; Schosseler, F. *Phys. Rev. Lett.* **1985**, *55*, 1110.